Pushing the Limits: Down-Converting Er^{3+}-Doped BaF_2 Single Crystals with Photoluminescence Quantum Yield Surpassing 100%

Eduard I. Madirov, Sergey V. Kuznetsov, Vasilii A. Konyushkin, Dmitry Busko, Bryce S. Richards, and Andrey Turshatov*

Down-conversion (DC) is a phenomenon that can enable the observation of photoluminescent quantum yield (PLQY) values exceeding 100%. A comprehensive study of the DC properties of BaF_2–based single crystals with different Er^{3+} doping levels (1–25 mol.%) is presented. The samples exhibit a PLQY of 110% in the 1550–1650 nm under 405 nm excitation. This remarkable PLQY is attributed to a cross-relaxation process within the energy levels of Er^{3+}. Furthermore, when considering all emitted photons in the 1000–1650 nm range, the PLQY reaches 153% for a sample doped with 5 mol.% of Er^{3+}. By integrating the emission of this single crystal with a Ge diode, serving as an example of a photovoltaic device sensitive to short-wave infrared light, a significant enhancement in short-circuit current is demonstrated. In a broader context, the presented material holds promise for improving the spectral response of low-bandgap photovoltaic devices.

1. Introduction

The trivalent erbium (Er^{3+}) ion is a commonly employed luminescent species to realize efficient up-conversion (anti-Stokes) emission.[1] However, its intricate energy level structure also suggests the potential for an inverse process whereby the absorption

of a single high-energy photon can lead to the emission of multiple lower energy photons,[2] such that a photoluminescent quantum yield (PLQY) – the ratio of the emitted and absorbed photons – of greater than unity is observed.

The terminology is often unclear in the literature. The term down-shifting (DS) or luminescent down-shifting (LDS) is usually used as a general name for any process in which the energy of the emitted photon is less than that of the excitation photon and the PLQY always remains ≤ 100%.[3–5]

The present authors define quantum-cutting (QC) to be the process whereby one absorbed higher-energy photon results in the emission of two or more lower-energy photons (PLQY can exceed 100%).[6] This process can be realized in several different ways.[7] The first one involves QC via the host lattice sites. Within this process, due to impact ionization the host lattice sites allow the generation of multiple lower-energy electron-hole pairs for each incident higher-energy photon. Certain luminescent materials, such as europium-doped yttrium oxide (Y_2O_3:Eu^{3+}), have exhibited remarkable PLQY for visible emission reaching an impressive value of 240%.[8] However, achieving such high PLQY required an extreme excitation energy of 23 eV (corresponding to a wavelength of 54 nm). In addition, an energy of at least 15 eV (83 nm) was necessary to attain PLQY surpassing unity.[8]

The second type is the QC on single ions where multiple photons are emitted in a stepwise manner. This mechanism becomes feasible due to the narrow energy levels of rare-earth ions separated by large energy gaps. While predicted by Dexter in 1957,[9] this was first experimentally observed using deep ultraviolet (UV) excitation of Pr^{3+}-doped fluoride-based crystals by two groups in 1974, resulting in a PLQY of 140%.[10] The process begins with the absorption of a 185 nm photon by the YF_3 host lattice. The absorbed energy is then transferred to the lower-lying $^1S_0$ state of Pr^{3+} via a 4f-5d transition. Following this, a blue photon (408 nm) is emitted via the $^1S_0$-$^1I_6$ transition, while a red photon (620 nm) is emitted via the $^3P_0$-$^3H_6$ transition. These results were determined via a relative PLQY measurement – non-ideal given today's reliance on absolute PLQY techniques.[11]

The term down-conversion (DC) is misused in the literature, sometimes meaning QC while on other occasions simply LDS. To avoid confusion, the present authors define the term "DC" in

E. I. Madirov, D. Busko, B. S. Richards, A. Turshatov
Institute of Microstructure Technology
Karlsruhe Institute of Technology
Hermann-von-Helmholtz-Platz 1, 76344 Eggenstein-Leopoldshafen, Germany
E-mail: andrey.turshatov@kit.edu
S. V. Kuznetsov, V. A. Konyushkin
Prokhorov General Physics Institute of the Russian Academy of Sciences
Vavilov Str, 38, Moscow 119991, Russia
B. S. Richards
Light Technology Institute
Karlsruhe Institute of Technology
Engesserstrasse 13, 76131 Karlsruhe, Germany

**ADVANCED
SCIENCE NEWS**

www.advancedsciencenews.com

**ADVANCED
OPTICAL
MATERIALS**

www.advopticalmat.de
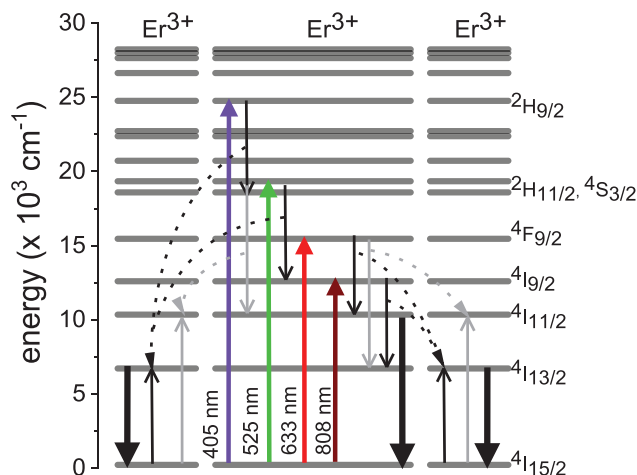
Figure 1. Energy level diagram of an Er^{3+} ion with possible mechanisms of DC and cross-relaxation between Er^{3+} ions.

a manner consistent with the definition used by Meijerink and co-workers,[7,12,13] referring to a process whereby the emission of multiple lower-energy photons (PLQY can exceed 100%) is achieved via cross-relaxation between two ions. This mechanism originated in the 1950s when Dexter formulated the concept of achieving two-photon emission through energy transfer,[9] and it can be treated as the opposite of the energy transfer up-conversion (ETU) process.[14]

QC materials were originally pursued for enhancing the brightness of Xe lamps and hence the interest in UV-to-visible processes.[15] In contrast, DC materials exhibit great potential for enhancing the efficiency of solar cells[7,16] and here a UV/visible-to-near-infrared (NIR) is favored. The diagram in **Figure 1** illustrates the possible ways to achieve DC from the visible to the NIR spectral range in the Er^{3+} ions.

There are already some published works devoted to the search of rare earth – doped QC materials that exhibit PLQY exceeding 100%. In the work[2] the authors reported the quantum efficiency of 190% in the $LiGdF_4$ powders doped with 0.5 mol.% of Eu^{3+} due to two-step process under 202 nm excitation of the ^6G_J level of Gd^{3+}.

Another system that is capable of efficient DC is the pair of Pr^{3+} and Yb^{3+} ions.[17,18] Although measurements of luminescence decays supported the DC mechanism in this material, achieving a PLQY exceeding 100% was not demonstrated, likely due to both concentration quenching and back energy transfer from Yb^{3+} to Pr^{3+}, contributing to the decrease in Yb^{3+} emission intensity. The work[19] showed that the PLQY of the Yb^{3+} emission in the Pr^{3+} and Yb^{3+} co-doped glasses and glass ceramics containing LaF_3 nanocrystals equals to 12% under 480 nm excitation. This result was obtained with a direct method for measurement of PLQY using an integrating sphere. It's interesting to note that the brightness (though not the PLQY) of the Pr^{3+} and Yb^{3+} co-doped $NaYF_4$ nanocrystals can be enhanced by the addition of Coumarin dye to increase the absorption cross-section in the blue spectral range.[20]

Another ion that can make DC possible is Tm^{3+}. Paper[21] was dedicated to the study of the 1800 nm emission of the Tm^{3+} doped $Gd_2O_2S:Tm^{3+}$ powders. UV, visible, and near-infrared excitation

photons can be converted to four, three, and two 1800 nm photons, respectively, in the sample with 10% mol.% of Tm^{3+}. Other papers[22,23] were dedicated to the study of the Tm^{3+}/Yb^{3+} co-doped systems. The first one[22] showed that in the lanthanum aluminum germanate glasses quantum efficiency of the Yb^{3+} emission under 467 nm excitation can reach 159.9%, whereas in the second one[23] Yb^{3+} quantum efficiency in the Tm^{3+}/Yb^{3+} co-doped YPO_4 powders was found to be 172.8% under 474 nm excitation. It's worth noting that, in both cases, the quantum efficiency values were derived through an analysis of the Tm^{3+} decay within a series of samples, rather than being directly measured using an integrating sphere.

Another promising approach to achieve QC involves doping rare earth ions into a perovskite host. Using the absolute method, it was determined that PLQY of Yb^{3+} emission in $CsPbCl_3$ nanocrystals reached 200% when excited at 405 nm.[16] Similar results are reported in the work[24] where Yb^{3+} ions were doped into the $CsPb(Cl_{1-x}Br_x)_3$ (x = 0.0, 0.41, 0.65, 0.87, and 1.0) host and excited with 365 nm light. Additionally, QC in Er^{3+} and Yb^{3+} doped $CsPbCl_3$ perovskite thin films were analyzed in.[25] Absolute quantum yield measurements demonstrated that under 300 nm excitation the luminescence quantum yield of either Er^{3+} or Yb^{3+} emission (at ≈980 nm) can exceed 100% depending on the concentration ratio of the doping ions.

The results presented above indicate that there are various approaches to QC and DC. It is also evident that different methods can be used to assess the efficiency of QC and DC processes. Two main techniques can be highlighted. One uses the change in the luminescence decay time of the donor state to obtain the efficiency of the energy transfer process, which then allows calculating QC(DC) PLQY. The second one relies on absolute PLQY measurement with a setup built around an integrating sphere that allows to explicitly estimate of the number of absorbed and emitted photons.

Similar to Tm^{3+}, the energy levels of the Er^{3+} ion offer multiple pathways to achieve DC with an efficiency exceeding 100%. However, the targeting of the transition between the first excited state $^4I_{13/2}$ and the ground state $^4I_{15/2}$ (≈1540 nm) appears to be the most favorable choice, supported by several key factors. First, this is due to the absence of alternative radiative pathways for energy dissipation at this level. Second, the substantial energy gap between the $^4I_{13/2}$ and $^4I_{15/2}$ states, exceeding 6500 cm^{-1}, surpasses the typical phonon energies of crystalline hosts, which are < 1000 cm^{-1}, making multiphonon relaxation an unlikely bridge. Third, as illustrated in Figure 1, numerous cross-relaxation routes are evident, facilitating the population of the $^4I_{13/2}$ state from higher-lying energy levels. It is clear from Figure 1 that different excitation wavelengths can enable the attainment of DC with varying efficiencies. Additionally, in the context of Er^{3+} ions, DC depends on cross-relaxation interactions among different Er^{3+} ions.[26,27] Therefore, the concentration of the Er^{3+} ions is expected to notably affect the probability of this process.

Beyond the choice of the luminescent ion (Er^{3+}), the selection of the host material plays a pivotal role in shaping the performance of the DC material. The host material must exhibit low phonon energy to minimize non-radiative losses and facilitate the desired radiative transitions. Recent studies have underscored the significance of MF_2 (M = Ca, Sr, Ba, Pb) as a family of host

**ADVANCED
SCIENCE NEWS**

www.advancedsciencenews.com

**ADVANCED
OPTICAL
MATERIALS**

www.advopticalmat.de

materials possessing these crucial properties.[28–31] Given its very low maximum phonon energy of 240 cm^{-1}, BaF$_2$ stands out as a promising candidate for use as a DC material.

So far, there are no reports that demonstrate absolute measurements of PLQY of the $^4I_{13/2} - {}^4I_{15/2}$ transition in the Er^{3+} ions that exceed 100%. Additionally, the majority of the reported PLQY values that do surpass 100% are obtained under either UV or vacuum ultraviolet (VUV) excitation in the samples co-doped with Er^{3+} and Yb^{3+}, yielding emission at 1500 nm.[25,32] Therefore, questions persist regarding the performance of samples solely doped with Er^{3+} when excited in the visible range. In this particular scenario, BaF$_2$ is selected as the host due to the aforementioned favorable characteristics. Furthermore, there have been no reported studies on the impact of (DC using Er^{3+} ions on the performance of photovoltaic (PV) systems. To address this objective, a germanium (Ge) photodiode is utilized as a model device to assess the enhancement in photocurrent, employing BaF$_2$:Er^{3+} single crystal as an illustrative example of a spectral conversion material. This decision is driven by the alignment of the Er^{3+} ion's emission band, centered ≈1540 nm, with the characteristics of PV devices.

Several research papers have proposed the use of erbium (Er^{3+})-doped DC materials to improve the efficiency of photovoltaic devices. For example, Huang et al. theoretically determined in their work[33] that the DC quantum efficiency in Er^{3+}:NaYF$_4$ nanostructured glass-ceramic could reach up to 150% under 485 nm excitation. The authors propose that after 485 nm excitation the excitation non-radiatively relaxes to the $^4S_{3/2}$ level of Er^{3+} from which there is a two-step process $^4S_{3/2} \rightarrow {}^4I_{9/2}$, $^4I_{9/2} \rightarrow {}^4I_{13/2}$ which leads to the population of the $^4I_{13/2}$ state. Each of these steps is resonant with the $^4I_{13/2} \rightarrow {}^4I_{15/2}$ transition which in total yields up to three emission photons after absorption of a single excitation quant. They suggested that this material has the potential to reduce energy losses in Si—Ge solar cells, thereby increasing their overall efficiency.

In another study by Elleuch et al.,[34] Er^{3+}-doped ZnO/Si thin films were proposed as both antireflective and DC materials for Si solar cells. It is proposed that after absorption of a 515 nm photon the $^4F_{7/2}$ level of Er^{3+} ion is populated. Then the emission of two 980 nm photons is achieved via the $^4F_{7/2} + {}^4I_{15/2} \rightarrow {}^4I_{11/2} + {}^4I_{11/2}$ and cross relaxation. In addition, Aouaini et al.[35] investigated Er^{3+}-doped tellurite glass as a luminescent material for solar concentrators, estimating a quantum efficiency of 91% for the $^4I_{13/2}$ emission band under 488 nm excitation. The authors suggest that after absorption of a 488 nm photon that populates the $^4F_{7/2}$ state there is a number of transitions ($^4S_{3/2} + {}^4I_{15/2} \rightarrow {}^4I_{9/2} + {}^4I_{13/2}$, $^4F_{7/2} + {}^4I_{15/2} \rightarrow {}^4F_{9/2} + {}^4I_{13/2}$, $^4F_{9/2} + {}^4I_{15/2} \rightarrow {}^4I_{11/2} + {}^4I_{13/2}$, $^4F_{7/2} + {}^4I_{15/2} \rightarrow {}^4I_{11/2} + {}^4I_{11/2}$ as well as $^4I_{9/2} + {}^4I_{15/2} \rightarrow {}^4I_{13/2} + {}^4I_{13/2}$) that can lead to the population of the $^4I_{13/2}$ state and subsequent emission of the 1.53 um photon.

Several other works, as referenced in[36] and[37] have also suggested the use of Er^{3+}/Yb^{3+} co-doped materials to improve the performance of Si solar cells. In both works cross-relaxation processes, such as Er^{3+}:($^4S_{3/2}$)+ Yb^{3+}:($^2F_{7/2}$)→ Er^{3+}:($^4I_{11/2}$)+ Yb^{3+}:($^2F_{5/2}$) lead to a population of the $^2F_{5/2}$ state of the Yb^{3+} and following emission of the photons with the wavelength around 1 um. However, it's worth noting that none of these papers provided experimental evidence with measured PLQY exceeding 100%, so the real impact of Er^{3+}-doped materials on the perfor-

mance of photovoltaic devices has yet to be conclusively demonstrated.

2. Results and Discussion

A typical emission spectrum of a BaF$_2$ crystal doped with 12 mol.% of Er^{3+} ions when excited with 405 nm light is presented in **Figure 2a**. The spectrum consists of a number of emission bands that correspond to the transitions in Er^{3+} ion, namely $^4S_{3/2} - {}^4I_{15/2}$ (545 nm), $^4F_{9/2} - {}^4I_{15/2}$ (660 nm), $^4S_{3/2} - {}^4I_{13/2}$ (850 nm), $^4I_{11/2} - {}^4I_{15/2}$ (990 nm), and $^4I_{13/2} - {}^4I_{15/2}$ (1550 nm). The most intense emission band is $^4I_{13/2} - {}^4I_{15/2}$ followed by $^4I_{11/2} - {}^4I_{15/2}$, with the remaining shorter-wavelengths bands being much weaker.

To determine the optimal doping concentration, the PLQY values were assessed in all single crystal samples. The resulting data is depicted in Figure 2b–d. The values in the Figure 2b illustrate that under 405 nm excitation some samples — specifically those doped with 5 and 12 mol.% of Er^{3+} ions— exhibit PLQY values surpassing unity (104 and 110%, respectively) for the $^4I_{13/2} - {}^4I_{15/2}$ emission band. This observation confirms the presence of the DC process in BaF$_2$:Er^{3+} crystals. However, for Er^{3+} concentrations below 5% and above 12%, the PLQY values are notably below unity. A similar concentration-dependent trend (with the optimum concentration of 10%) was previously observed for Gd$_2$O$_2$S:Tm^{3+} samples.[21] The authors of the work[21] observed that at considerably lower concentrations, cross-relaxation is outweighed by radiative or non-radiative relaxation, whereas at significantly higher concentrations, luminescence decreases due to concentration quenching – a process involving the migration of excitation across the Tm^{3+} sublattice until it encounters a quenching site.

Under 525 nm excitation, PLQY of the $^4I_{13/2} - {}^4I_{15/2}$ band reaches 92% in the sample doped with 5 mol.% of Er^{3+}, but fails to surpass unity. It is interesting to note that in the samples with lower doping concentration (< 5 mol.%), 405 nm excitation provides lower PLQY values than upon 525 nm. In the case of 405 nm excitation, the Er^{3+} ion is excited to the $^2H_{9/2}$ state. Unlike $^2H_{11/2}$ state to which the ion is excited with a 525 nm excitation, energy gaps in the 25 000–17 000 cm^{-1} region are rather small (<2000 cm^{-1}) and can be bridged by a number of phonons which makes multiphonon relaxation probable.[38] Thus, in the samples with lower doping concentration under 405 nm excitation cross-relaxation competes with multiphonon processes leading to lower PLQY values.

At two other studied excitation wavelengths, 633 and 808 nm, much lower PLQY values are achieved, reaching 35% and 46%, respectively. These excitation wavelengths may not be favorable for cross-relaxation with the population of the $^4I_{13/2}$ level, offering fewer opportunities for the DC process compared to the 405 and 525 nm excitations.

In addition to this data, it is worth studying the PLQY of the state $^4I_{13/2}$ under direct excitation. In this case, a 1510 nm laser diode is used. The values in Figure 2b show that in the samples with doping concentration lower than 5 mol.% the PLQY is close to unity. This means that concentration quenching is only present in the samples with doping higher than 5 mol.%. These

ADVANCED
SCIENCE NEWS
www.advancedsciencenews.com

ADVANCED
OPTICAL
MATERIALS
www.advopticalmat.de
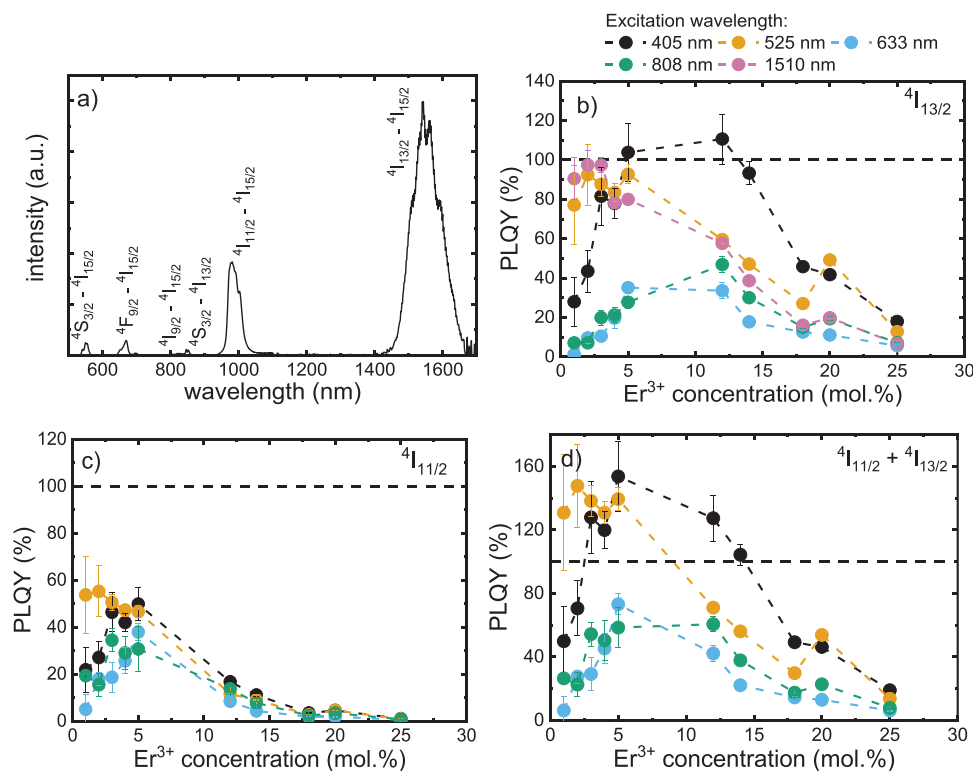
Figure 2. a) Emission spectrum of the BaF_2:Er (12 mol.%) sample under 405 nm excitation; PLQY of the b) $^4I_{13/2} - {}^4I_{15/2}$ c) $^4I_{11/2} - {}^4I_{15/2}$, d) total NIR emission of the BaF_2:Er^{3+} single crystals under different visible range excitation.

findings are in line with previous research into quenching of the NIR emission of Er^{3+} ions.[39,40]

The second most intense radiative energy relaxation channel is the $^4I_{11/2} - {}^4I_{15/2}$ transition. This emission can be also harvested to enhance the response of the systems sensitive to NIR radiation. The PLQY values (Figure 2c) can go as high as 50%, which shows that a significant portion of the excitation energy leaves the system this way. The concentration dependence of the $^4I_{13/2} - {}^4I_{15/2}$ band PLQY has a similar trend as one of the $^4I_{13/2} - {}^4I_{15/2}$ band. The values go up until the concentration reaches 5–12 mol.% at which point the highest PLQY is observed. Further increase in the doping concentration leads to a drop in the observed values. This demonstrates that under all studied excitation wavelengths a similar fraction of the absorbed energy escapes via $^4I_{11/2} - {}^4I_{15/2}$ transition.

In order to better understand the effect of the doping concentration on the PLQY of the $^4I_{11/2} - {}^4I_{15/2}$ emission band the PLQY of this band was obtained under direct (976 nm) excitation. The results are presented in Figure S3b (Supporting Information). The PLQY of the $^4I_{11/2}$ luminescence exhibits a notable upward trend within the concentration range of 1% to 4%. This can be attributed to the increasing rate of the radiative transition. It is worth noting that a similar effect, where the absorption cross sections (and rate of radiative transitions) of Yb^{3+} and Er^{3+} increases with an increase in Ln^{3+} concentration, has previously been observed in our research on BaF_2 and PbF_2 single crystals, as documented in our previous work.[29,30]

In order to further study the effect of concentration on radiative transition probabilities the luminescence decay times of

the $^4I_{13/2}$, $^4I_{11/2}$, $^4F_{9/2}$ as well as $^4S_{3/2}$ states are obtained and the results are presented in Figure S4 (Supporting Information). The lower-lying levels ($^4I_{13/2}$ and $^4I_{11/2}$) experience a decrease in the luminescence decay time mostly due to concentration quenching.[41] The higher energy levels ($^4F_{9/2}$ and $^4S_{3/2}$) also show a noticeable decrease in luminescence decay time with increasing Er^{3+} concentration. While cross-relaxation plays a role in this decrease, it is important to recognize that other factors, such as an increased emission rate and concentration quenching, could contribute to the phenomenon.

If the emission of the two NIR emission bands is summed (Figure 2d) then the total PLQY of a number of samples exceeds unity – namely crystals doped with 3–14 mol.% in the case of 405 nm excitation and ones doped with 1–5 mol.% under 525 nm excitation. The highest value (153%) is observed in the sample doped with 5 mol.% of Er^{3+} under 405 nm excitation.

It is also worth mentioning that a part of the excitation relaxes via the emission in the visible spectral range. Compared to the NIR emission (see Figure 2a) visible emission accounts for a small fraction of total yield (Figure S2a, Supporting Information). Integration of the emission spectra in the broad range of 410–1700 nm at 405 nm excitation leads to the highest PLQY of 160% for the sample with 12 mol.% concentration of Er^{3+}.

In summary, the following trends in the PLQY concentration dependence can be observed. Under 405, 633, and 808 nm excitation, the PLQY of both $^4I_{13/2}$ and $^4I_{11/2}$ emission bands increases with concentration up to 12 mol%, where the highest values are observed. As the doping concentration is further increased, the PLQY values decrease. Under 525 nm excitation, there is little

**ADVANCED
SCIENCE NEWS**

www.advancedsciencenews.com

**ADVANCED
OPTICAL
MATERIALS**

www.advopticalmat.de
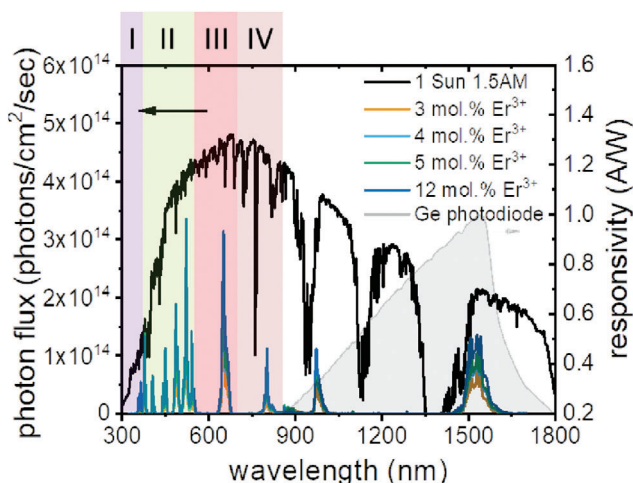
Figure 3. AM1.5G solar spectrum (black) as well as the number of solar photons absorbed by 3–12 mol.% Er^{3+}-doped BaF_2 crystals. The colored bands I–IV represent spectral regions selected for calculation of the number of emitted photons, while the spectral response of the Ge photodiode is plotted in grey.

change in the PLQY values of both bands in the concentration range 1–5 mol.%. Increasing the concentration above 5 mol% leads to a decrease in the observed values.

This remarkable efficiency in spectral conversion offers diverse potential applications. Low bandgap (<0.8 eV) photovoltaic devices are most often used as a part of multijunction solar cells.[42,43] The most common semiconductor is Ge,[44] but there are also GaInNAsSb,[45–47] GaSb[48] and solar cells based on PbS colloidal quantum dots[49] among others. These photovoltaic materials have the highest responsivity in the ≈1500 nm region while being unresponsive to the visible part of the spectrum. Combination with a material that is capable of efficient conversion of visible emission into NIR (1400–1700 nm) range can extend their spectral responsivity and increase the efficiency. On top of that thermophotovoltaic systems that are tuned to utilize the emission of a blackbody at around 1800 K[50–52] can also gain from such spectral conversion materials.

If the intended use of the material pertains to photovoltaics, its performance should be evaluated under excitation intensities equivalent to solar illumination. To assess the practical efficacy of BaF_2:Er^{3+} crystals, the change in the short-circuit current of a commercially available Ge-photodiode was calculated under 1 Sun illumination conditions when combined with the studied crystals. The choice of a Ge-photodiode as the representative photovoltaic system was influenced by its spectral response aligning with the $^4I_{13/2} - ^4I_{15/2}$ emission band of Er^{3+} ions. For subsequent analysis, four BaF_2 crystals (doped with Er^{3+} ions at concentrations of 3, 4, 5, and 12 mol.%) – which exhibited the highest quantum yield values – were selected. Additionally, due to the PLQY values being close to 100% under 1510 nm excitation the emission reabsorption should not cause any significant losses in these samples.

Figure 3 shows the AM1.5G solar spectrum as well as the absorbed photon count by the investigated crystals under 1 Sun (1000 W m^{-2}) intensity. This data is used to estimate the enhance-

ment in the performance of PV devices that the DC in crystals can provide.

To calculate the number of photons emitted in the NIR range by the crystals, the visible range of the solar spectrum is partitioned into four segments. It is assumed that the PLQY of the crystals remains consistent within the respective ranges. The PLQY within band I is assumed to be equivalent to the estimate under 405 nm excitation, within band II – under 525 nm, band III – under 633 nm, and band IV – under 808 nm excitation. By determining the absorbed photon count and establishing PLQY, it becomes possible to deduce the number of photons emitted within the NIR spectral range. Combining this value with the established spectral response of a Ge-photodiode enables the computation of the short-circuit current yielded by spectral conversion within the crystals. One more additional factor should be also taken into account. The crystal's emission is isotropic. Therefore, when it is positioned atop a Ge-photodiode, we should take into account that only approximately half of the emitted photons can effectively reach the photovoltaic device. Thus, when calculating the short-circuit current only half of the number of the emitted photons should be considered.

The results of the calculations presented in **Figure 4a** show that the maximum projected enhancement in short-circuit current density (J_{SC}) amounts to 0.67 mA cm^{-2} in the case of the crystal doped with 5 mol.% of Er^{3+}. In order to put this value into some context, the current generated in the Ge photodiode by the NIR (>850 nm) part of the solar spectrum is estimated.

The spectral response of the Ge-diode is taken from the manufacturer's website[53] and is presented in Figure 3. In order to obtain the J_{sc} under solar irradiation the following assumptions are made. First, the AM1.5G solar spectrum is recalculated from photons/s/cm^2 into W/s/cm^2 yielding the data in Figure S5 (Supporting Information). Then this spectrum is multiplied by the aforementioned responsivity of the Ge-photodiode and the resulting values are integrated giving the value of 6 mA cm^{-2}. With this in mind, it can be calculated that the enhancement is up to 11% of the initial current.

The proposed setup for the measurement of J_{sc} enhancement is presented in (Figure 4b). Er^{3+} doped BaF_2 crystals are placed on top of the Ge – photodiode with silicon oil serving as the refractive index matching liquid. The images of the device captured in the visible and short-wave infrared ranges are presented in Figure S6 (Supporting Information). The whole assembly is then placed under a solar simulator and the J–V curves are obtained. The data is presented in Figure S7 (Supporting Information).

Adding an undoped BaF_2 crystal increases the observed Jsc due to the improved light coupling. In the 1500 nm region, the refractive index of Ge is ≈4.21, whereas the refractive index of BaF_2 is 1.46 and silicon oil is 1.41. The change to the J_{sc} that the doped crystals introduce is calculated in relation to the measurement with an undoped crystal. The highest value of the J_{sc} enhancement (0.6 mA cm^{-2}) is detected when the crystal doped with 12 mol.% of Er^{3+} ions is used.

When comparing the experimental results to the calculations it should be noted that even though there is a refractive index matching liquid (silicon oil) between the crystal and photodiode some boundary reflections are still present as well as waveguiding in the crystal that can help the emission to escape through the crystal sides and lead to loss of emission. For example, the

**ADVANCED
SCIENCE NEWS**

www.advancedsciencenews.com

**ADVANCED
OPTICAL
MATERIALS**

www.advopticalmat.de
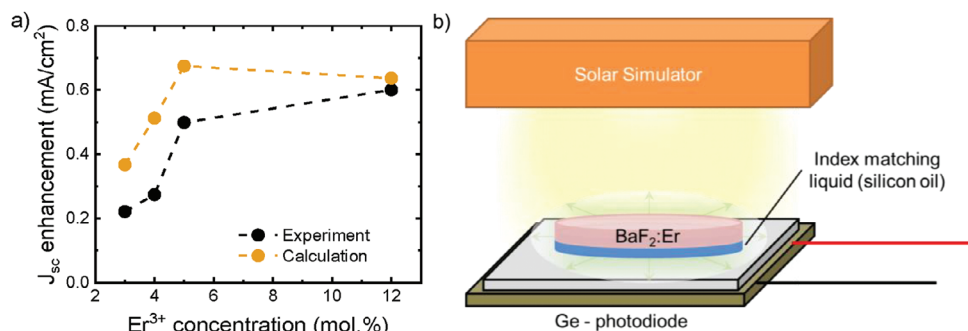
Figure 4. a) Measured and calculated short-circuit current density enhancement; b) setup for the estimation of the enhancement of the short-circuit current of the Ge – photodiode

phenomenon of waveguiding is readily evident in the photograph depicted in Figure S8 (Supporting Information). In this case, the obtained results exhibit reasonable agreement with the predictions.

3. Conclusion

It is demonstrated that down-shifting phenomena can allow observing DC PLQY values exceeding unity. The highest DS PLQY value of $^4I_{13/2} - {}^4I_{15/2}$ transition is 110% while the sum of the $^4I_{13/2} - {}^4I_{15/2}$ and $^4I_{11/2} - {}^4I_{15/2}$ transitions is 153%. These values are found in the BaF_2 crystal doped with 5 mol.% of Er^{3+} ions under 405 nm excitation. As well as this, the change in the J_{sc} of a Ge-photodiode combined with Er^{3+}-doped BaF_2 crystals is evaluated both theoretically and experimentally under solar irradiation. The highest detected enchantment is 0.6 mA cm^{-2}.

4. Experimental Section

Ten BaF_2-based single crystals doped with different concentrations of Er^{3+} ions (1, 2, 3, 4, 5, 12, 14, 18, 20, 25 mol.%) were grown in a vacuum with a fluorinating atmosphere (CF_4) by Bridgman technique as detailed elsewhere.[29,54,55] The crystals were cut and polished to yield discs with 10 mm diameter with a thickness of 1.7 mm. The actual content of the Er^{3+} ions in the crystals is estimated based on the XRD data and is presented in Table S1 (Supporting Information).

The absolute PLQY values were obtained with a setup built around an integrating sphere (Labsphere, Ø6'', 3 P-LPM-060-SL) that has been described earlier.[29,30] The excitation sources are laser diodes: 405 nm (Roithner, DL-7146-1012S), 525 nm (Roithner, LD-515-10MG), 633 nm (Roithner, ADL-63302TL), 808 nm (Thorlabs, L808P200), and 1510 nm (RLT1510-20MGS-B, Roithner). The detectors are NIR (Ocean Insight, NIRQuest, 900–1700 nm) and UV–Vis–NIR (Thorlabs, CCS200/M, 200 – 1000 nm) spectrometers. The absorption data was obtained with a UV–Vis–NIR spectrophotometer (Cary 7000, Agilent). For determining the solar conversion efficiency, current density – voltage (J-V) curves of the Ge photodiode (Thorlabs, FDG10 × 10) were obtained using a source-meter (Keithley, 2450) and a solar-simulator (Wavelabs, Sinus 70) that provided a very good match to the air-mass 1.5 global solar spectrum over the 350– 1260 nm range. A hyperspectral image of the device in the short-wave infrared range was captured using a Specim FX17 camera.

Luminescence lifetimes of the emissive levels were measured with a home-built optical system described previously.[29] Briefly, 525, 633, 976, and 1510 nm (Roithner) laser diodes mounted in temperature stabilized mounts (TCLDM9, Thorlabs) and driven by a laser diode controller (ITC4001, Thorlabs) were used as the excitation sources. The lumi-

nescence wavelength was selected with a double monochromator (Bentham, DTMS300) and the signal was detected with a photomultiplier tube (R928P, Hamamatsu) mounted in a temperature-cooled housing (CoolOne, Horiba) in the UV–Vis region or with an infrared single-photon detector (ID Quantique, ID220) in IR region-both detectors were coupled to the multi-channel scaling card (TimeHarp 260, Picoquant). In order to exclude the effects of reabsorption on the detected decay time, the decays were obtained from the powder samples prepared as follows. Parts of the studied crystals were ground to powder and then mixed with barium sulphate, which was optically inactive in the Vis–NIR region. The ratio of the Er^{3+}-doped BaF_2 to the $BaSO_4$ is 1 to 9.

Supporting Information

Supporting Information is available from the Wiley Online Library or from the author.

Conflict of Interest

The authors declare no conflict of interest.

Data Availability Statement

The data that support the findings of this study are available from the corresponding author upon reasonable request.

[1] B. S. Richards, D. Hudry, D. Busko, A. Turshatov, I. A. Howard, *Chem. Rev.* **2021**, *121*, 9165.

[2] R. T. Wegh, H. Donker, K. D. Oskam, A. Meijerink, *J. Lumin.* **1999**, *82*, 93.

[3] M. D. Dramićanin, *Methods Appl. Fluoresc.* **2016**, *4*, 042001.

[4] D. Alonso-Álvarez, D. Ross, E. Klampaftis, K. R. McIntosh, S. Jia, P. Storiz, T. Stolz, B. S. Richards, *Prog. Photovoltaics* **2015**, *23*, 479.

[5] H. J. Hovel, R. T. Hodgson, J. M. Woodall, *Sol. Energy Mater.* **1979**, *2*, 19.

[6] W. Zhu, D. Chen, L. Lei, J. Xu, Y. Wang, *Nanoscale* **2014**, *6*, 10500.

[7] B. S. Richards, *Sol. Energy Mater. Sol. Cells* **2006**, *90*, 1189.

[8] J. K. Berkowitz, J. A. Olsen, *J. Lumin.* **1991**, *50*, 111.

[9] D. L. Dexter, *Phys. Rev.* **1957**, *108*, 630.

[10] W. W. Piper, J. A. DeLuca, F. S. Ham, *J. Lumin.* **1974**, *8*, 344.

[11] E. Madirov, D. Busko, F. A. Cardona, D. Hudry, S. V. Kuznetsov, V. A. Konyushkin, A. N. Nakladov, A. A. Alexandrov, I. A. Howard, B. S. Richards, A. Turshatov, *Adv. Photonics Res.* **2022**, *4*, 2200187.

[12] K. D. Oskam, R. T. Wegh, H. Donker, E. V. D. van Loef, A. Meijerink, *J. Alloys Compd.* **2000**, *300*, 421.

[13] R. T. Wegh, H. Donker, E. V. D. van Loef, K. D. Oskam, A. Meijerink, *J. Lumin.* **2000**, *87*, 1017.

[14] F. Auzel, *Chem. Rev.* **2004**, *104*, 139.

[15] T. Jüstel, H. Nikol, C. Ronda, *Angew. Chem., Int. Ed.* **1998**, *37*, 3084.

[16] C. S. Erickson, M. J. Crane, T. J. Milstein, D. R. Gamelin, *J. Phys. Chem. C* **2019**, *123*, 12474.

[17] L. Aarts, B. v. d. Ende, M. F. Reid, A. Meijerink, *Spectrosc. Lett.* **2010**, *43*, 373.

[18] S. V. Kuznetsov, O. A. Morozov, V. G. Gorieva, M. N. Mayakova, M. A. Marisov, V. V. Voronov, A. D. Yapryntsev, V. K. Ivanov, A. S. Nizamutdinov, V. V. Semashko, P. P. Fedorov, *J. Fluorine Chem.* **2018**, *211*, 70.

[19] Y. Xu, X. Zhang, S. Dai, B. Fan, H. Ma, J.-l. Adam, J. Ren, G. Chen, *J. Phys. Chem. C* **2011**, *115*, 13056.

[20] Z. Wang, A. Meijerink, *J. Phys. Chem. Lett.* **2018**, *9*, 1522.

[21] D.-C. Yu, R. Martín-Rodríguez, Q.-Y. Zhang, A. Meijerink, F. T. Rabouw, *Light: Sci. Appl.* **2015**, *4*, e344.

[22] Q. Zhang, B. Zhu, Y. Zhuang, G. Chen, X. Liu, G. Zhang, J. Qiu, D. Chen, *J. Am. Ceram. Soc.* **2010**, *93*, 654.

[23] L. Xie, Y. Wang, H. Zhang, *Appl. Phys. Lett.* **2009**, *94*, 061905.

[24] D. M. Kroupa, J. Y. Roh, T. J. Milstein, S. E. Creutz, D. R. Gamelin, *ACS Energy Lett.* **2018**, *3*, 2390.

[25] A. Ishii, T. Miyasaka, *J. Chem. Phys.* **2020**, *153*, 194704.

[26] L. Tao, W. Xu, *Appl. Phys. Express* **2013**, *6*, 092301.

[27] Y. Wang, Z. You, J. Li, Z. Zhu, E. Ma, C. Tu, *J. Phys. D: Appl. Phys.* **2009**, *42*, 215406.

[28] D. Saleta Reig, B. Grauel, V. A. Konyushkin, A. N. Nakladov, P. P. Fedorov, D. Busko, I. A. Howard, B. S. Richards, U. Resch-Genger, S. V. Kuznetsov, A. Turshatov, C. Würth, *J. Mater. Chem. C* **2020**, *8*, 4093.

[29] E. I. Madirov, V. A. Konyushkin, A. N. Nakladov, P. P. Fedorov, T. Bergfeldt, D. Busko, I. A. Howard, B. S. Richards, S. V. Kuznetsov, A. Turshatov, *J. Mater. Chem. C* **2021**, *9*, 3493.

[30] E. Madirov, D. Busko, I. A. Howard, B. S. Richards, A. Turshatov, *Phys. Chem. Chem. Phys.* **2023**, *25*, 11986.

[31] M. Zong, Y. Wang, Z. Zhang, J. Liu, L. Zhao, J. Liu, L. Su, *J. Lumin.* **2022**, *250*, 119089.

[32] R. T. Wegh, E. V. D. van Loef, A. Meijerink, *J. Lumin.* **2000**, *90*, 111.

[33] X. Huang, D. Chen, L. Lin, Z. Wang, Z. Feng, Z. Zheng, *Optik* **2014**, *125*, 565.

[34] R. Elleuch, R. Salhi, S. I. Al-Quraishi, J. L. Deschanvres, R. Maâlej, *Phys. Lett. A* **2014**, *378*, 1733.

[35] F. Aouaini, A. Maaoui, N. B. H. Mohamed, M. M. Alanazi, L. A. El Maati, *J. Alloys Compd.* **2022**, *894*, 162506.

[36] M. Bouzidi, A. Maaoui, N. Chaaben, A. S. Alshammari, Z. R. Khan, M. Mohamed, *J. Non-Cryst. Solids* **2022**, *595*, 121837.

[37] A. Verma, S. K. Sharma, *Ceram. Int.* **2017**, *43*, 8879.

[38] Y. V. Orlovskii, K. K. Pukhov, T. T. Basiev, T. Tsuboi, *Opt. Mater.* **1995**, *4*, 583.

[39] F. Chen, T. Wei, X. Jing, Y. Tian, J. Zhang, S. Xu, *Sci. Rep.* **2015**, *5*, 10676.

[40] S. Jia, C. Li, Z. Zhao, C. Yao, Z. Jia, G. Qin, Y. Ohishi, W. Qin, *ACS Mater. Lett.* **2018**, *227*, 97.

[41] Z. Mazurak, *Opt. Mater.* **1993**, *2*, 101.

[42] M. Yamaguchi, T. Takamoto, K. Araki, N. Ekins-Daukes, *Sol. Energy* **2005**, *79*, 78.

[43] A. Aho, A. Tukiainen, V. Polojärvi, M. Guina, *Nanoscale Res. Lett.* **2014**, *9*, 61.

[44] C. Baur, M. Meusel, F. Dimroth, A. W. Bett, presented at Conf. Record of the Thirty-first IEEE Photovoltaic Specialists Conf., Lake Buena Vista, Florida, January, **2005**, https://doi.org/10.1109/PVSC.2005.1488185.

[45] R. Isoaho, T. Aho, A. Aho, A. Tukiainen, J. Reuna, M. Raappana, M. Guina, *Sol. Energy Mater. Sol. Cells* **2022**, *234*, 111413.

[46] R. Isoaho, A. Tukiainen, J. Puutio, A. Hietalahti, J. Reuna, A. Fihlman, E. Anttola, M. Keränen, A. Aho, M. Guina, *Sol. Energy Mater. Sol. Cells* **2022**, *248*, 111987.

[47] R. Isoaho, A. Aho, A. Tukiainen, T. Aho, M. Raappana, T. Salminen, J. Reuna, M. Guina, *Sol. Energy Mater. Sol. Cells* **2019**, *195*, 198.

[48] P. Gupta, Y. Kim, J. Im, G. Kang, A. M. Urbas, K. Kim, *ACS Appl. Energy Mater.* **2021**, *4*, 9304.

[49] Y. Bi, A. Bertran, S. Gupta, I. Ramiro, S. Pradhan, S. Christodoulou, S.-N. Majji, M. Z. Akgul, G. Konstantatos, *Nanoscale* **2019**, *11*, 838.

[50] C. Ferrari, F. Melino, M. Pinelli, P. R. Spina, M. Venturini, *Energy Procedia* **2014**, *45*, 160.

[51] S. Bitnar, W. Durisch, G. Palfinger, F. von Roth, U. Vogt, A. Brönstrup, D. Seiler, *Semic* **2004**, *38*, 941.

[52] J. van der Heide, N. E. Posthuma, G. Flamand, J. Poortmans, *AIP Conf. Proc* **2007**, *890*, 129.

[53] Thorlabs, FDG10X10 – Ge Photodiode, https://www.thorlabs.com/thorproduct.cfm?partnumber=FDG10X10 (accessed: March 2024).

[54] B. P. Sobolev, N. L. Tkachenko, *J. Less-Common Met.* **1982**, *85*, 155.

[55] S. V. Kuznetsov, P. P. Fedorov, *Inorg. Mater.* **2008**, *44*, 1434.